

---

# **Final Project Report**

## **SEIRD Modelling of Highly Pathogenic Avian Influenza (HPAI)**



---

Joanne GIBERT

Zoé JACOB

December 17, 2025

## Contents

<b>1</b>	<b>Introduction</b>	<b>2</b>
<b>2</b>	<b>Deviations from project proposal</b>	<b>2</b>
<b>3</b>	<b>Approach and model</b>	<b>3</b>
3.1	SEIRD model formulation . . . . .	3
3.2	C implementation and numerical solver . . . . .	5
3.3	MATLAB automation . . . . .	5
<b>4</b>	<b>Results</b>	<b>6</b>
4.1	SEIRD curves across scenarios . . . . .	6
4.2	Effective reproduction number $R_{\text{eff}}$ . . . . .	6
4.3	Summary metrics . . . . .	7
<b>5</b>	<b>Discussion</b>	<b>9</b>
5.1	Effects of transmission, recovery, and mortality on SEIRD dynamics . . . . .	9
5.2	Why doesn't the epidemic start in scenario 1 ? . . . . .	11
5.3	Why is the epidemic slower for scenario 4 ? . . . . .	11
<b>6</b>	<b>Conclusion</b>	<b>12</b>

## 1 Introduction

Poultry farming has become increasingly important to meet the demands of a growing population, which has led to the expansion of intensive farming practices. However, in high-density farms, where chicken are kept in close quarters, certain diseases spread more easily. One such disease is Highly Pathogenic Avian Influenza (HPAI), which can devastate an avian population, killing between 75% and 100% of individuals [1]. Understanding how environmental and farm-management factors influence outbreak severity is essential for improving disease mitigation strategies.

Our model is based on 3 varying parameters: the recovery rate  $\gamma$ , the transmission rate  $\beta$ , and the mortality rate  $\mu$ . The objective of this project is to simulate different epidemiological scenarios by changing  $\gamma$ ,  $\beta$  and  $\mu$ . These variations allow us to model conditions such as heatwaves, high population density, and a decrease in mortality. We model the disease using a SEIRD framework, where individuals transition between five compartments: Susceptible (S), Exposed (E), Infected (I), Recovered (R), and Deceased (D).

How do changes in the transmission rate  $\beta$ , recovery rate  $\gamma$ , and mortality rate  $\mu$  affect the dynamics of HPAI outbreaks in a closed poultry population?

## 2 Deviations from project proposal

Our initial proposal described the development of a SEIRD model to evaluate the influence of the transmission rate  $\beta$  and the recovery rate  $\gamma$  on HPAI. Instead of simulating only six scenarios as originally proposed, we extended our analysis to nine scenarios, summarized in Table 1, in order to also explore the effect of altering the mortality rate  $\mu$ . The choice of the parameters is described in Section 3.1.

Table 1: Summary of simulation scenarios.

Scenario	$\gamma$ [day $^{-1}$ ]	$\beta$ [day $^{-1}$ ]	$\mu$ [day $^{-1}$ ]	$R_0$
1	0.10	0.40	0.30	1
2	0.10	0.80	0.30	2
3	0.10	1.20	0.30	3
4	0.05	0.40	0.30	1.14
5	0.05	0.80	0.30	2.29
6	0.05	1.20	0.30	3.43
7	0.10	0.40	0.033	3
8	0.10	0.80	0.033	6
9	0.10	1.20	0.033	9

### 3 Approach and model

#### 3.1 SEIRD model formulation

We implemented the classical SEIRD model defined by the following system of differential equations [2]:

$$\frac{dS}{dt} = -\beta \frac{SI}{N} \quad (1)$$

$$\frac{dE}{dt} = \beta \frac{SI}{N} - \sigma E \quad (2)$$

$$\frac{dI}{dt} = \sigma E - (\gamma + \mu)I \quad (3)$$

$$\frac{dR}{dt} = \gamma I \quad (4)$$

$$\frac{dD}{dt} = \mu I \quad (5)$$

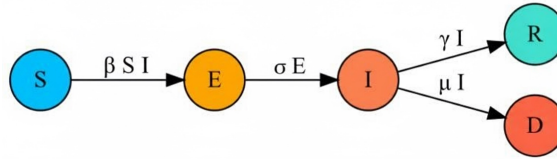


Figure 1: SEIRD epidemiological model diagram.

The simulation is conducted under nine scenarios, combining different recovery, transmission and mortality conditions (Table 1). All the parameters were selected based on values from epidemiological literature.

- $\beta$  = **transmission rate**. It represents the rate at which a susceptible individual becomes infected after contact with an infected individual. The unit of  $\beta$  is day<sup>-1</sup>. For example, if  $\beta = 0.4$  day<sup>-1</sup>, this means that each infected individual infects 0.4 new individuals per day on average. We considered three values of  $\beta$ : 0.4, 0.8 and 1.2 day<sup>-1</sup>, to simulate population density [5]. High  $\beta$  represents high population density.
- $\sigma$  = **incubation rate**. It represents the rate at which exposed individuals become infectious. The unit of  $\sigma$  is day<sup>-1</sup>. The quantity  $1/\sigma$  corresponds to the average incubation period. For HPAI in poultry farming, it is approximately 14 days [3]. Therefore,  $\sigma = 1/14 \approx 0.07$  day<sup>-1</sup> means that about 7% of exposed individuals progress to the infectious stage each day.
- $\gamma$  = **recovery rate**. It represents the rate at which infected individuals recover. The unit of  $\gamma$  is day<sup>-1</sup>. The quantity  $1/\gamma$  corresponds to the average infectious period. For example, if  $\gamma = 0.1$  day<sup>-1</sup>, it means that around 10% of infected individuals recover each day. We considered two values of  $\gamma$ : 0.1 and 0.05 day<sup>-1</sup>. Indeed, the infectious period of HPAI is around 10 days for normal conditions [4]. Furthermore, several physiological studies show

that heat reduces antibody production and delays immune responses, leading to significantly longer recovery times [6]. For modelling purposes, this effect is represented by multiplying the infectious period by 2 during heatwave scenarios, or in other words: dividing the recovery rate  $\gamma$  by 2, hence  $\gamma = 0.05 \text{ day}^{-1}$ .  $1/\gamma$  is the mean infectious period in the absence of mortality, as defined by the model. However, when death is possible, the actual mean time an individual remains infectious is  $1/(\gamma + \mu)$ , which will later be used to discuss the results in Section 5.

- $\mu = \mathbf{mortality\ rate}$ . It represents the rate of death due to infection. The unit of  $\mu$  is  $\text{day}^{-1}$ . For example, if  $\mu = 0.3 \text{ day}^{-1}$ , it means that 30% of infected individuals die each day. We considered two values of  $\mu$ : 0.3 and  $\frac{1}{30} \approx 0.033 \text{ day}^{-1}$ . The justification for these values is given below.
- $R_0 = \mathbf{basic\ reproduction\ number}$ . It represents the average number of secondary infections caused by one infectious individual in a fully susceptible population. It is a dimensionless number. In the SEIRD model, it can be expressed as:

$$R_0 = \frac{\beta}{\gamma + \mu}$$

$R_0$  does not appear directly in the equations but is useful to understand the parameters more easily. We will also use the effective reproduction number  $R_{\text{eff}}$ , which accounts for the fraction of the population that is still susceptible and provides a dynamic measure of transmission during the course of the epidemic.

- $I_0 = \mathbf{initial\ number\ of\ infected\ individuals}$ . We initialise the system with a single infected bird ( $I_0 = 1$ ), representing the introduction of the virus into an otherwise fully susceptible flock. All remaining individuals begin in the susceptible compartment, and no birds start exposed, recovered, or deceased.
- $N = \mathbf{total\ population\ size}$ . We choose  $N = 10,000$  as a representative population size. This value is realistic for large commercial poultry houses, as Swiss farms can reach up to about 18,000 birds [8]. We use the frequency-dependent transmission term  $\beta SI/N$ , so fixing  $N$  does not change the qualitative dynamics.

The infection fatality ratio (IFR) of HPAI in chickens ranges between 75% and 100% [1]. We first set it to 75% to allow room for comparison with other parameters. In the SEIRD model, the IFR must satisfy:  $\frac{\mu}{\mu+\gamma} = 0.75$ . If we keep  $\gamma = 0.1 \text{ day}^{-1}$  then  $\mu = 0.3 \text{ day}^{-1}$ .

When a heatwave occurs,  $\gamma$  is divided by 2:  $\gamma = 0.05 \text{ day}^{-1}$ , while  $\mu$  remains constant. As a result, the infection fatality ratio increases because individuals recover more slowly, even though their daily mortality risk does not change ( $\mu$  stays the same).

We also consider a hypothetical, milder HPAI scenario with an IFR of 25%, imagining that the chicken population has developed better immunity to the virus. Keeping  $\gamma = 0.1 \text{ day}^{-1}$  and imposing  $\frac{\mu}{\mu+\gamma} = 0.25$  gives  $\mu = \frac{1}{30} \approx 0.033 \text{ day}^{-1}$ .

Finally, all the varying parameters are summarized in Table 1 and the constant parameter values are :

$$\sigma = \frac{1}{14} \approx 0.07 \text{ day}^{-1} \quad N = 10,000 \quad I_0 = 1$$

### 3.2 C implementation and numerical solver

The system was solved using the Euler forward method implemented in C. The program:

- reads all parameter sets from `parameters.csv`,
- initializes the SEIRD state with one infected individual ( $I_0 = 1$ ),
- performs time stepping over 2000 simulated days with  $dt = 0.1$ ,
- writes each scenario to a file `scenario_i.csv` ( $i = 1, \dots, 9$ ).

We also solved the differential equations in MATLAB (the code we wrote for this purpose doesn't appear in the final MATLAB script), which confirmed that our curves were correct.

### 3.3 MATLAB automation

MATLAB automates the entire analysis:

1. calls the C executable to generate all scenario files;
2. reads all `scenario_*.csv` files;
3. computes:
  - peak infected individuals,
  - total deaths individuals,
  - time to decline (first day when  $R_{\text{eff}} < 1$  permanently),
  - time to end (first day when  $E$  and  $I$  remain  $< 1$  permanently);
4. generates:
  - SEIRD time-series plots for each scenario,
  - full-scale view of scenario 4 dynamics,
  - effective reproduction number  $R_{\text{eff}}$  plots,
  - summary table of time metrics and population metrics (in .csv)
  - summary bar charts of time metrics and population metrics.

This approach ensures complete reproducibility: running the MATLAB script regenerates all figures and summary metrics.

## 4 Results

### 4.1 SEIRD curves across scenarios

Figure 2 provides an overview of the full SEIRD dynamics for all nine scenarios, showing how the susceptible, exposed, infectious, recovered, and deceased compartments evolve over time. Each panel corresponds to one parameter set and illustrates how changes in transmission, recovery, and mortality reshape the epidemic trajectory, from no outbreak in scenario 1 to fast, high-peak epidemics in scenarios 7 to 9. A detailed analysis of these curves is provided in Section 5.

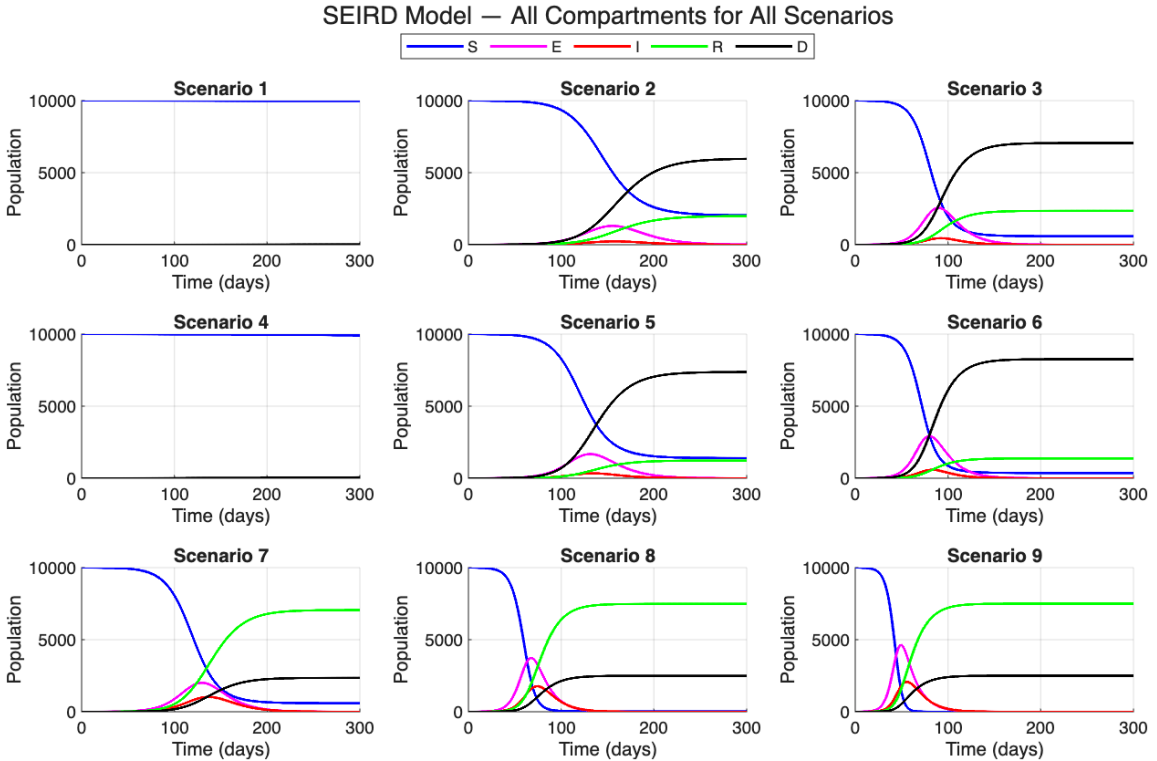


Figure 2: SEIRD dynamics for all scenarios.

### 4.2 Effective reproduction number $R_{\text{eff}}$

Let's introduce the concept of epidemic threshold. The epidemic threshold is a critical boundary in infectious disease dynamics that determines whether a disease will spread through a population or die out. This threshold is defined by the effective reproduction number  $R_{\text{eff}}$  [7]. The effective reproduction number,

$$R_{\text{eff}}(t) = \frac{\beta \cdot S(t)}{(\gamma + \mu)N},$$

is shown in Figure 3. The epidemic threshold occurs at  $R_{\text{eff}} = 1$ :

- $R_{\text{eff}} < 1$  : each infected individual produces fewer than 1 secondary infection on average, therefore the epidemic cannot sustain itself and dies out.
- $R_{\text{eff}} = 1$  : each infected individual produces exactly one secondary infection on average (critical threshold).
- $R_{\text{eff}} > 1$  : each infected individual produces more than 1 secondary infection on average, therefore the epidemic can spread exponentially.

Indeed, identifying the time  $t$  at which  $R_{\text{eff}}$  falls below 1 is important to determine the onset of its decline and to compare it with other scenarios (see time to decline in Figure 5).

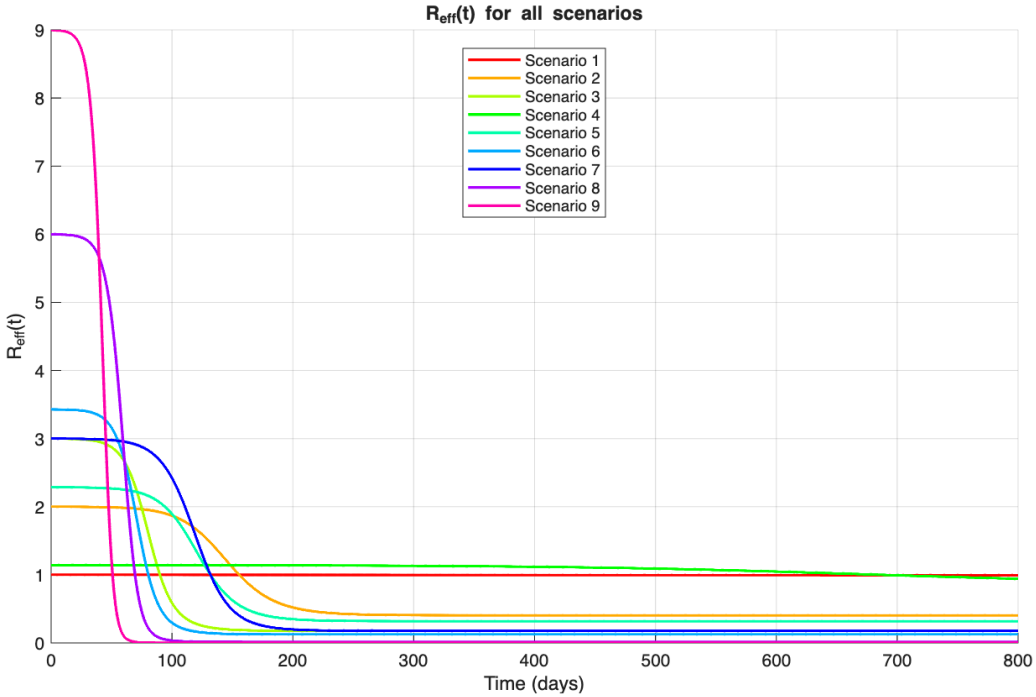


Figure 3:  $R_{\text{eff}}(t)$  for all scenarios.

### 4.3 Summary metrics

The key metrics across scenarios are visualized in Figures 4 for population metrics and 5 for time metrics. Calculating two different “end times” is interesting because it separates the beginning of control from the effective extinction of the epidemic. Having both times allows us to quantify when interventions or immunity start to “bend” the curve and how long residual transmission continues afterwards, which is important for planning control measures and evaluating scenario differences. Specifically, scenarios 5 and 7 share the same time to decline (131.9 days) because they have the same  $\beta$  (0.8 day<sup>-1</sup>). However, their time to end differs because mortality is higher in scenario 5 than in scenario 7, which means that even after the epidemic starts to decline, the way individuals leave the infectious and exposed compartments differs, leading to a longer period before  $E$  and  $I$  stay permanently below 1 in scenario 5.

In the population metrics in Figure 4, peak infected and total deaths generally increase with higher transmission rates  $\beta$  or lower recovery rates  $\gamma$ , with scenarios 2 to 6 up to about 8,300 deaths, while scenarios 7 to 9 produce very large peaks of infection (between 1,000 and 2,000 individuals) but fewer deaths (around 2,500). These differences are due to the decrease of the mortality rate  $\mu$  ( $0.3 \text{ day}^{-1}$  for scenarios 1 to 6 compared to  $0.033 \text{ day}^{-1}$  for scenarios 7 to 9).

In the timing metrics in Figure 5, time to decline (first day with  $R_{\text{eff}} < 1$  permanently) typically ranges between about 50 and 160 days, whereas time to end (first day from which  $E < 1$  and  $I < 1$  permanently) extends from roughly 175 to 370 days, except for scenario 4 where the epidemic is extremely prolonged (decline at 687 days and end at 1389 days).

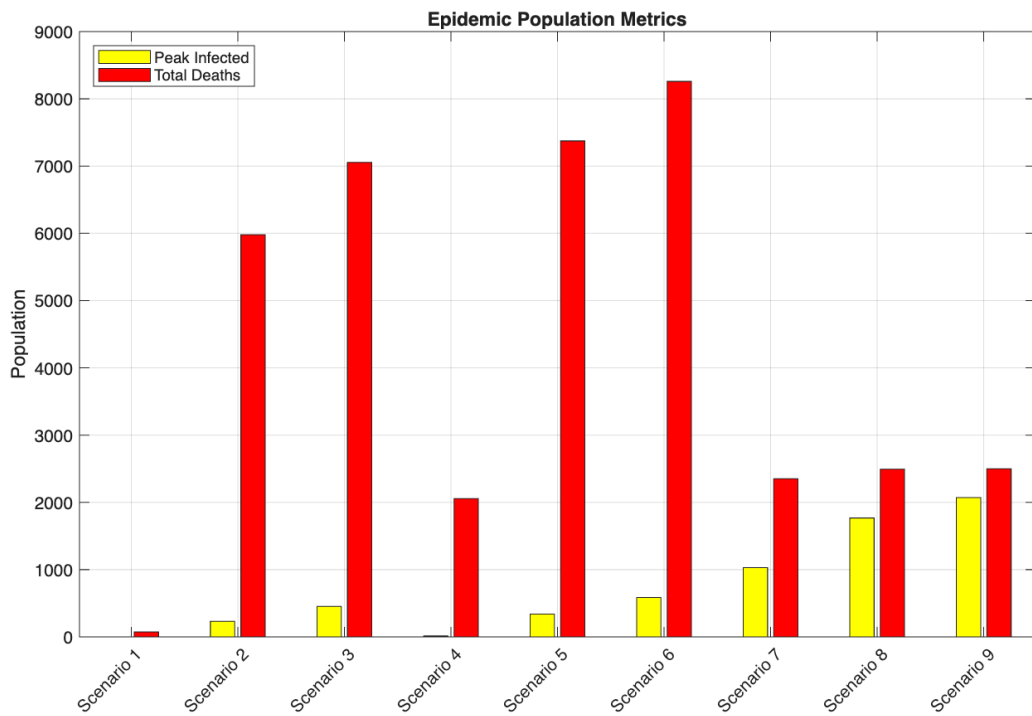


Figure 4: Peak infected individuals and total deaths for each scenario.

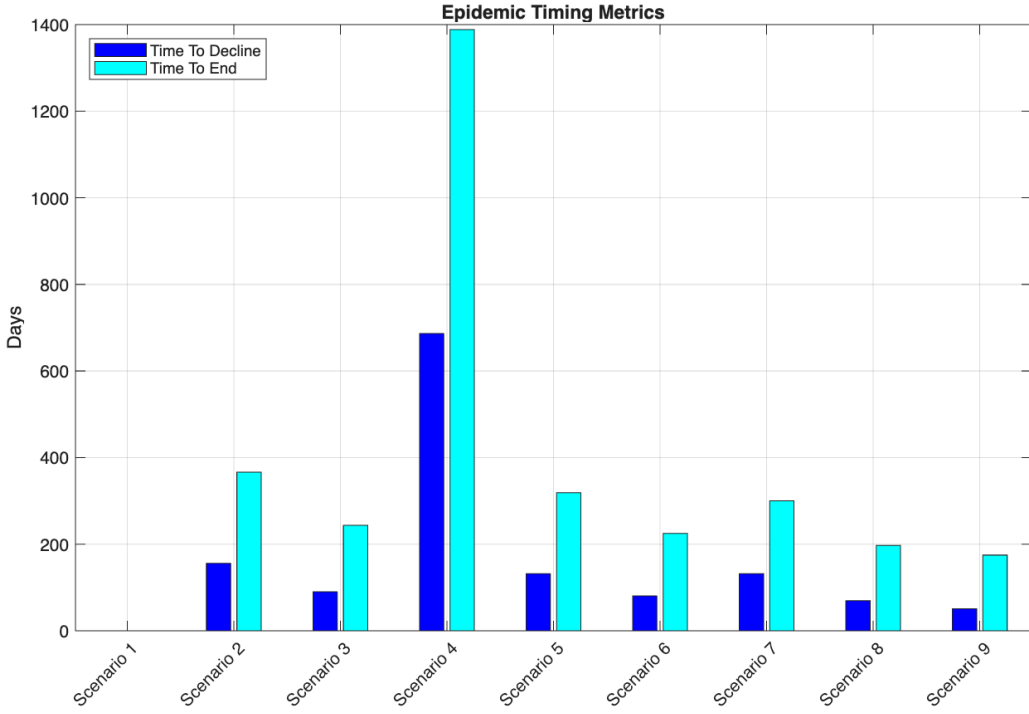


Figure 5: Time to decline and time to end.

A full numerical summary is available in `summary_results.csv`.

## 5 Discussion

### 5.1 Effects of transmission, recovery, and mortality on SEIRD dynamics

The SEIRD curves in Figure 2 clearly show how transmission rate  $\beta$ , recovery rate  $\gamma$ , and mortality rate  $\mu$  jointly shape the progression of HPAI outbreaks.

In scenarios 1 to 3, where  $\gamma$  and  $\mu$  are constant but  $\beta$  increases, the epidemic peak becomes progressively higher and earlier, illustrating the strong amplifying effect of population density on outbreak intensity. Scenario 1 ( $R_0 = 1$ ) exhibits no real epidemic, while scenarios 2 and 3 ( $R_0 = 2$  and 3) show increasingly rapid depletion of susceptible and a rise in infections. This trend is further confirmed in Figure 4, where the peak infected population increases substantially from scenario 2 to scenario 3. Additionally, Figure 5 shows how increasing  $\beta$  shortens the time to decline, as transmission rapidly drives  $R_{\text{eff}}(t)$  below 1 (Figure 3).

Scenarios 4 to 6 replicate the same  $\beta$  values but under heatwave conditions ( $\gamma$  halved). Interestingly, halving the recovery rate from  $\gamma = 0.1$  to  $\gamma = 0.05 \text{ day}^{-1}$  does not systematically lead to much longer epidemics in scenarios 5 and 6. This is because removal from the infectious compartment is dominated by mortality: with  $\mu = 0.3 \text{ day}^{-1}$ , the total exit rate is  $\gamma + \mu = 0.4 \text{ day}^{-1}$  at normal

temperature, and  $\gamma + \mu = 0.35 \text{ day}^{-1}$  during a heatwave. Consequently, the mean infectious period increases only slightly, from  $\frac{1}{0.4} = 2.5 \text{ days}$  to  $\frac{1}{0.35} \approx 2.86 \text{ days}$ , which is far from a twofold increase despite  $\gamma$  being halved. This explains why in Figure 5, scenarios 5 and 6 do not show longer times to decline or end compared to scenarios 2 and 3, even though their infected curves appear slightly higher in Figure 2.

In contrast, the infection fatality ratio (IFR) is strongly affected. At normal temperature, the IFR satisfies

$$\text{IFR} = \frac{\mu}{\mu + \gamma} = \frac{0.3}{0.3 + 0.1} = 0.75,$$

whereas during a heatwave it becomes

$$\text{IFR} = \frac{0.3}{0.3 + 0.05} \approx 0.86.$$

Thus, in our simulations, reducing  $\gamma$  mainly increases mortality. Figure 4 clearly illustrates this effect: scenario 5 and especially scenario 6 exhibit substantially higher total deaths than their normal-temperature counterparts (scenarios 2 and 3). It also produces a noticeably higher infectious peak, since the higher IFR reduces the rate at which infected birds leave the infectious compartment through recovery. However, this effect is not strong enough to substantially extend the overall duration of the epidemic, except in scenario 4 where  $R_0$  is only slightly above the epidemic threshold. This is also reflected in both Figure 3, where scenario 4 maintains  $R_{\text{eff}}(t)$  above 1 longer than any other scenario, and Figure 5, which shows its exceptionally long time to decline and extinction (see Section 5.3).

Finally, scenarios 7 to 9 examine the impact of reducing mortality to  $\mu = 0.033 \text{ day}^{-1}$  while keeping  $\gamma = 0.1 \text{ day}^{-1}$ . Because  $\mu$  enters the denominator of  $R_0 = \beta/(\gamma + \mu)$ , lowering  $\mu$  dramatically increases  $R_0$  (3, 6, and 9 respectively). As a result, infections spread explosively even at low  $\beta$ , producing very large I and E peaks. This is reflected in Figure 4, where peak infected values increase sharply across scenarios 7 to 9. Unlike the earlier scenarios, however, most individuals eventually recover rather than die, leading to a dominant recovered population and minimal mortality. The rapid depletion of susceptibles also explains why, as seen in Figure 5, the time to decline is slightly shorter in scenarios 8 and 9: the epidemic grows so explosively that  $R_{\text{eff}}(t)$  drops below 1 earlier simply because the susceptible population collapses much faster. Moreover, decreasing  $\mu$  accelerates the start of the epidemic, since a lower mortality rate reduces the total removal rate ( $\gamma + \mu$ ), allowing infected individuals to remain infectious longer and increasing the early effective reproduction number, as seen in Figure 3. These scenarios illustrate how a less lethal strain can still produce a much larger epidemic due to increased transmission potential.

Together, these nine simulations demonstrate three major trends: transmission rate  $\beta$  primarily controls the size and speed of the outbreak, recovery rate  $\gamma$  shapes the severity of the epidemic mainly through its impact on the infection fatality ratio, while mortality rate  $\mu$  determines the final distribution between recovered and deceased individuals. Figures 3, 4, and 5 together reinforce these conclusions by showing coherent patterns across effective reproduction numbers, epidemic

magnitude, and epidemic duration. The model therefore captures distinct biological mechanisms influencing HPAI severity under varying environmental and evolutionary conditions.

## 5.2 Why doesn't the epidemic start in scenario 1 ?

The epidemic in scenario 1 never takes off because the effective reproduction number is exactly at the epidemic threshold ( $R_0 = 1$ ). Moreover, the effective reproduction number  $R_{\text{eff}}$  seems to stay constant as seen in Figure 3. In this situation, each infected individual generates on average one new infection, so the number of infectious individuals cannot grow exponentially. Moreover, the high mortality rate ( $\mu = 0.3 \text{ day}^{-1}$ ) removes infected chickens from the population quickly, while the relatively low transmission rate ( $\beta = 0.4 \text{ day}^{-1}$ ) does not allow them enough time to infect others before dying. As a result, the infection fails to propagate and effectively “burns itself out,” with mortality outpacing the creation of new secondary cases.

## 5.3 Why is the epidemic slower for scenario 4 ?

Scenario 4 exhibits much slower epidemic dynamics, extending to nearly 1500 days (about more than 4 years), as seen in Figure 6. This is because it operates just above the epidemic threshold, with  $R_0 = 1.14$ . Although  $R_{\text{eff}} > 1$  allows the epidemic to spread, this value is only slightly above the critical point, so the initial expansion of infection is extremely slow (see Figure 3 for the variations of  $R_{\text{eff}}$ ). The epidemic does eventually reach a substantial scale, but its progression unfolds over a far longer timeframe : nearly an order of magnitude slower than in scenarios with higher  $R_0$  values.

Nevertheless, this duration is of the same order as the natural lifespan of domestic chickens, which typically live around 5-10 years under good conditions [9]. As a result, scenario 4 should be interpreted as a mathematically valid but biologically extreme case: the infection lingers at low levels over almost an entire chicken lifetime, which is unlikely for a HPAI in real poultry populations, but useful to illustrate how dynamics slow down when  $R_0$  is only slightly above the epidemic threshold.

The reason the epidemic occurs in scenario 4 but not in scenario 1 is the difference in the recovery rate  $\gamma$ , since all other parameters are identical. Reducing  $\gamma$  in scenario 4 lowers the total removal rate ( $\gamma + \mu$ ), which increases the basic reproduction number to  $R_0 = 1.14$ . This slight increase is just enough to push the system above the epidemic threshold, allowing infections to grow, whereas Scenario 1 remains exactly at  $R_0 = 1$  and therefore cannot sustain an outbreak.

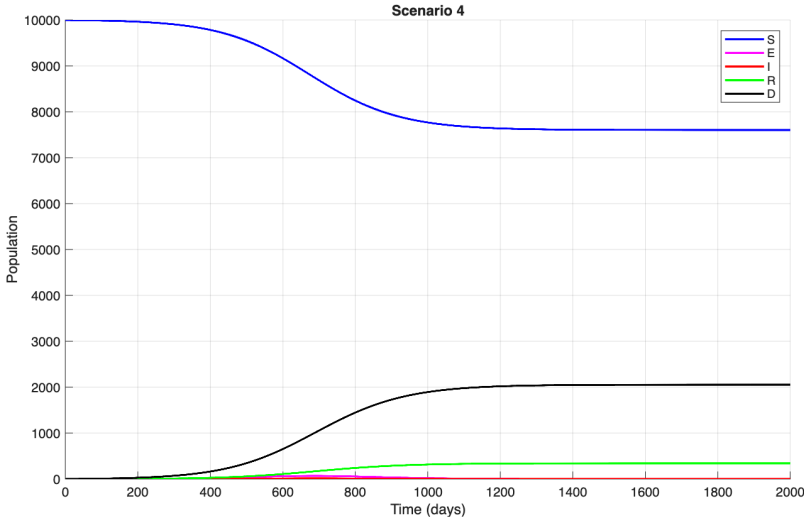


Figure 6: Full-scale view of Scenario 4

## 6 Conclusion

In this project, we developed a complete computational framework combining a C implementation of the SEIRD model with an automated MATLAB analysis in order to investigate how population density, temperature-dependent recovery, and mortality shape the dynamics of Highly Pathogenic Avian Influenza (HPAI) in poultry farms. By systematically varying the parameters  $\beta$ ,  $\gamma$ , and  $\mu$  across nine scenarios, we were able to isolate the individual and combined effects of these biological and environmental drivers.

Our results show that transmission rate  $\beta$ , which reflects contact intensity and therefore farm density, is the dominant factor controlling both the speed and magnitude of the outbreak. Higher values of  $\beta$  consistently produced earlier and larger infection peaks, as confirmed by the SEIRD curves and the peak-infection metrics. In contrast, changes in the recovery rate  $\gamma$  did not uniformly alter the duration of the epidemic. Because removal from the infectious compartment is strongly dominated by mortality, halving  $\gamma$  only slightly increased the infectious period, and therefore had limited impact on epidemic length except in scenario 4, where  $R_0$  lay just above the epidemic threshold. However, reducing  $\gamma$  markedly increased the infection fatality ratio, leading to substantially more deaths and higher infectious peaks. It should be emphasized that this framework is intended to provide qualitative insight into HPAI dynamics rather than precise predictions; indeed, some configurations, such as scenario 4, are deliberately less representative of real-world conditions and primarily serve to illustrate model sensitivities.

Finally, lowering the mortality rate  $\mu$  had two major effects: it dramatically increased  $R_0$ , resulting in explosive outbreaks, and it shifted the final composition of the population almost entirely toward recovery rather than death. These scenarios illustrate how a less lethal strain can nonetheless generate a far larger epidemic due to increased transmission potential.

Overall, our findings highlight the importance of understanding how environmental conditions and farm management practices interact with pathogen life-history traits. Even simple compartmental models such as SEIRD can provide valuable insights into HPAI dynamics, offering a quantitative basis for anticipating outbreak severity and evaluating mitigation strategies. Fortunately, Switzerland already enforces strict limits on flock size : 18 000 birds per facility, and sets strong minimum housing conditions such as space allowances [8]. Such measures contribute to reducing the risks highlighted in this study.

## Authorship statement

Both authors contributed equally to this project.

- **Joanne Gibert:** MATLAB automation, parameter selection, figure generation, interpretation of results, report writing, README file writing.
- **Zoé Jacob:** C model implementation, parameter selection, interpretation of results, references, report writing.

All components of the project and the final report were jointly reviewed and validated by both authors.

## References

- [1] Cornell University College of Veterinary Medicine. *Avian Influenza (Bird Flu) Fact Sheet*. In *Highly Pathogenic Avian Influenza (Bird Flu) Resource Center*. Retrieved from Cornell Vet website <https://www.vet.cornell.edu/highly-pathogenic-avian-influenza-bird-flu-resource-center/avian-influenza-bird-flu-fact-sheet>
- [2] H. J. Farm, S. A. van der Vegt, B. Lambert, *SEIRD model*, COMO-DTC Collaboration, 2025. Available online: <https://como-dtc-collaboration.github.io/como-models/articles/SEIRD.html>
- [3] World Organisation for Animal Health (WOAH). (2024). *Chapter 10.4 – Infection with high pathogenicity avian influenza viruses*. In *Terrestrial Animal Health Code*. Retrieved from [https://www.woah.org/fileadmin/Home/eng/Health\\_standards/tahc/2023/chapitre\\_avian\\_influenza\\_viruses.pdf](https://www.woah.org/fileadmin/Home/eng/Health_standards/tahc/2023/chapitre_avian_influenza_viruses.pdf)
- [4] Carsten Kirkeby, Anette Boklund, Lars Erik Larsen & Michael P. Ward, *Are all avian influenza outbreaks in poultry the same? The predicted impact of poultry species and virus subtype*, Zoonoses and Public Health, vol.71, no.3, pp.314–323, 2024. Available at: <https://onlinelibrary.wiley.com/doi/full/10.1111/zph.13116>
- [5] Lambert S., Bauzile B., Mugnier A., Durand B., Vergne T., Paul M.C., *A systematic review of mechanistic models used to study avian influenza virus transmission and control*, Veterinary Research, 2023. Available at: <https://pmc.ncbi.nlm.nih.gov/articles/PMC10585835/>

- [6] E. M. Oluwagbenga, *Heat stress and poultry production: a comprehensive review*, Poultry Science, 2023. Available at: <https://www.sciencedirect.com/science/article/pii/S0032579123006600>.
- [7] Health Knowledge, *Epidemic Theory*, Public Health Textbook. Available at: <https://www.healthknowledge.org.uk/public-health-textbook/research-methods/1a-epidemiology/epidemic-theory>
- [8] Bio Suisse. (n.d.). *L'élevage de poules dans le respect de l'espèce*. Bio Suisse. Récupéré de <https://www.bio-suisse.ch/fr/notre-engagement/bien-etre-animal/elevage/elevage-de-poules.html>
- [9] A. Lehr, *How Long Do Chickens Live?*, Grubbly Farms, 2023. Available at: <https://grubblyfarms.com/blogs/the-flyer/how-long-do-chickens-live>